

BIOCHEMISTRY OF THE SOLUBLE METHANE MONOOXYGENASE

John D. Lipscomb

Department of Biochemistry, Medical School, University of Minnesota,
Minneapolis, Minnesota 55455

KEY WORDS: oxygenase, *Methylosinus trichosporium* OB3b, oxygen activation, oxygen
bridged diiron cluster, Fe(IV), oxene intermediate

CONTENTS

INTRODUCTION	372
STRUCTURE	374
<i>Activity, Quaternary Structure, and Cofactor Content</i>	374
<i>Spectroscopic Studies of the Diiron Cluster of MMOH</i>	375
MECHANISM	378
<i>Chemical Approaches</i>	380
<i>Transient Kinetic Approaches</i>	383
THE ROLES OF REDUCTASE AND COMPONENT B IN THE CATALYTIC CYCLE	387
<i>Complex Formation</i>	388
<i>Product Distribution Studies</i>	392
<i>Hypothesis for Regulation</i>	394

ABSTRACT

The soluble form of methane monooxygenase (MMO) catalyzes the reaction $\text{NAD(P)H} + \text{O}_2 + \text{CH}_4 + \text{H}^+ \rightarrow \text{NAD(P)}^+ + \text{H}_2\text{O} + \text{CH}_3\text{OH}$. Many other hydrocarbons serve as adventitious substrates. MMO consists of three protein components: component B, reductase, and hydroxylase (MMOH), the active site of which contains a hydroxo-bridged dinuclear iron cluster that is the site of catalysis. Such a cluster has not been previously associated with oxygenases, and spectroscopic studies have been conducted to ascertain its structural features and accessibility. The mechanism of MMO has been investigated through the use of diagnostic chemical reactions and transient kinetics. Both approaches are consistent with a mechanism in which the diiron cluster is first reduced to

the diferrous state and then reacts with O_2 . The O-O bond is apparently cleaved heterolytically to yield water and an $[Fe(IV)\bullet Fe(IV)]=O$ species, which purportedly abstracts a hydrogen atom from methane to yield a substrate radical and a diiron cluster-bound hydroxyl radical. Recombination of the radicals yields the product methanol. An intermediate with the properties of the novel $[Fe(IV)\bullet Fe(IV)]=O$ species has been trapped and characterized. This is the first such species to be isolated in biology. Meanwhile, the reductase and component B have roles in catalysis beyond simple electron transfer from NAD(P)H. These roles appear to be related to regulation of catalysis, and are mediated by the formation of specific component complexes that alter the physical and catalytic properties of MMOH at different stages of the turnover cycle.

INTRODUCTION

Methanotrophic bacteria occupy a niche in lakes, oceans, and wet soils at the interface of the aerobic and anaerobic environments (34, 66). There they oxidize methane resulting from anaerobic metabolism as their sole source of carbon and energy (4). The oxidant for this process is molecular O_2 , and the only metabolic product released is CO_2 , which can be readily converted to biomass by other organisms. In this way, most of the atmospheric egress of biogenic methane in aqueous environments is prevented.

Figure 1 illustrates the pathway that has been advanced for methane metabolism by methanotrophs.

The enzymes from this pathway have all been isolated and characterized to varying extents (4, 5, 11, 16, 19, 36, 51, 69). Each enzyme catalyzes a two-electron oxidation of its substrate, but the biochemical mechanisms for these oxidation reactions are quite different. Together, they present a fascinating example of biological diversity and a challenge for researchers interested in biological oxidation/reduction mechanisms.

The pathway is initiated by methane monooxygenase (MMO) through a reaction that cannot be catalyzed efficiently by any other enzyme—the splitting of the stable C-H bond of methane (bond dissociation energy of 104 kcal/mol). MMO is a classic monooxygenase in that two reducing equivalents from NAD(P)H are required to split the O-O bond of O_2 . These reducing equivalents are segregated with one of the oxygen atoms to form H_2O , while the second oxygen atom is incorporated into methane to form CH_3OH with nearly 100% efficiency (10, 19). This stoichiometry is exhibited by other monooxygenases that catalyze oxidation of larger, more reactive hydrocarbons, notably the family of cytochrome P-450s (P-450) (44). However, MMO is unique in that its reactive center does not contain a heme cofactor or any of the other cofactors encountered previously in oxygenase chemistry. This chapter reviews the

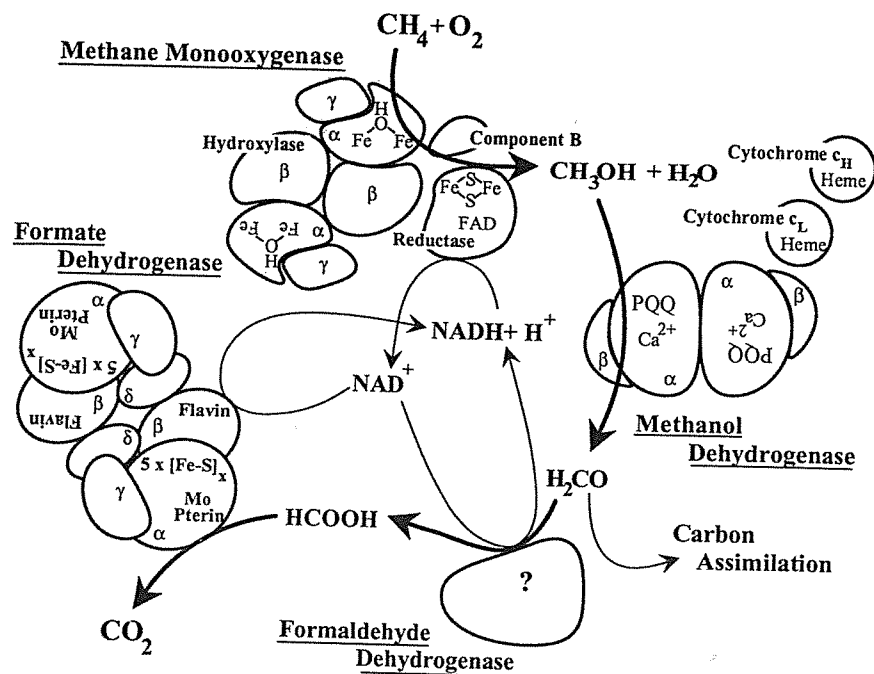


Figure 1 The four enzymes of the methane oxidation pathway of methanotrophic bacteria. The components and quaternary structures of the enzymes are shown as they are currently known. The quaternary structure and cofactor content of formaldehyde dehydrogenase is not known. In most cases, the specific subunit where cofactors bind is not known. The flavin present in formate dehydrogenase is similar but not identical to flavin mononucleotide (FMN) (36). PQQ is pyrroloquinoline quinone. The soluble form of MMO is illustrated. An equivalent pathway presumably exists for the methanotrophs expressing particulate MMO. (Compiled from Refs. 4, 5, 10, 11, 16, 19, 36, 51, 69).

unique structure of the active-site cofactor of MMO and the reaction-cycle chemistry that it catalyzes. It is demonstrated that the spectroscopic features and the kinetic characteristics of MMO combine to make it perhaps the best system in which to investigate the critical oxygen activation and insertion steps of the monooxygenase catalytic cycle.

Although methane is the only substrate that can support rapid growth,¹ MMO catalyzes adventitious oxidation of a broad range of other hydrocarbons (2, 9, 10, 18, 30, 34, 58, 64). These include saturated, unsaturated, linear,

¹Methanol will support slow growth; this has been exploited for the generation of mutations in the MMO genes (48).

branched, and cyclic hydrocarbons up to approximately C_8 in size. Also, single- and double-ring aromatics, heterocycles, halogenated alkenes, and ethers are turned over at a reasonable fraction of the rate of methane. Apparently, the very powerful oxidizing reagent generated in the active site of MMO to react with methane gives MMO the ability to catalyze the oxidation of most other hydrocarbons. The ability of MMO to catalyze the oxidation of many abundant and potentially toxic hydrocarbons has led industrial and environmental chemists to explore applications for its catalytic prowess. Moreover, structural and mechanistic studies of MMO have been greatly facilitated by its ability to bind and/or oxidize diagnostic substrates, inhibitors, and other small molecules.

MMO is also unique in that a single organism can harbor mutually exclusive soluble and particulate forms of the enzyme (4, 61, 64). The methanotrophs described over 20 years ago by Whittenbury and colleagues (66) are now divided into three classes based on their cell morphology and metabolic pathways. Type I methanotrophs possess only particulate MMO and utilize the condensation of ribulose 5-phosphate with formaldehyde to initiate carbon assimilation. Type II and type X methanotrophs elaborate either the soluble or the particulate form depending upon factors such as the culture cell density and the copper concentration of the growth media (61). Type X methanotrophs use the same carbon assimilation pathway as type I organisms, but the type II organisms use a unique pathway based upon the addition of formaldehyde to glycine to form serine. Only the soluble form of MMO has been purified to homogeneity (19, 20, 47, 52, 55, 67) (this review examines only this enzyme in detail). Recently, some progress was made in stabilizing the particulate enzyme in crude extracts (8). Preliminary characterizations suggest that it utilizes copper instead of iron. No reviews of the particulate form of MMO have appeared, but recent reviews of the soluble form of MMO are available (11, 22, 26, 28).

STRUCTURE

Activity, Quaternary Structure, and Cofactor Content

Soluble MMO has been purified to homogeneity from type X *Methylococcus capsulatus* (Bath) (10, 11, 55, 67), and type II *Methylosinus trichosporium* OB3b (19, 20), *Methylobacterium* species CRL-26 (52), and *Methylocystis* species M (47). The MMO from each source except *Methylobacterium* species CRL-26 consists of three protein components: hydroxylase (MMOH) (245 kDa) containing nonheme iron, component B (15.8 kDa) with no cofactors, and reductase (38.4 kDa) containing FAD and an $[Fe_2S_2]$ cluster (19). MMOH is a dimer of α , β , and γ subunit types (11, 19, 67). The *Methylobacterium* species CRL-26 reportedly consists of only reductase and MMOH (52). How-

ever, the similarity of this organism to *M. trichosporium* and spectroscopic characterizations suggest that all of the MMOs actually consist of three components.

Our initial work in this field (19) resulted in procedures that allowed the enzyme from *M. trichosporium* to be produced in high yield and with specific activities as much as 20 times greater than those reported for the other purified MMOHs. In contrast to these enzymes, the specific activity of the homogeneous *M. trichosporium* MMO as purified by our procedures is high enough to account for the growth rate of the organism. Consequently, the remainder of the discussion pertains to the MMO from this organism unless stated otherwise.

Spectroscopic Studies of the Diiron Cluster of MMOH

INITIAL CHARACTERIZATION The homogeneous MMOH is essentially colorless in the visible spectral region; this observation rules out the presence of heme, flavin, and iron-sulfur cofactors (19). Metal quantitations of the most active preparations of the enzyme showed that approximately four iron atoms were present. As isolated, MMOH exhibited no significant electron paramagnetic resonance (EPR) spectrum (25, 68). Mössbauer spectroscopy of protein prepared from bacteria grown in an ^{57}Fe -enriched medium (25) showed that all of the iron is inherently high spin Fe(III) ($S = 5/2$), but it is bound in antiferromagnetically coupled pairs $\{[\text{Fe(III)}\bullet\text{Fe(III)}]\}$ to yield the EPR silent, diamagnetic ($S = 0$) state. Upon one electron reduction, an EPR spectrum was observed at $g = 1.94, 1.86, 1.76$. Resonances in this range have only been reported for oxygen-bridged dinuclear iron clusters such as those found in the mixed valence states $\{[\text{Fe(II)}\bullet\text{Fe(III)}]\}$ of hemerythrin (62, 65) and uteroferrin (3). The cluster could be reduced by a second electron to eliminate the EPR signal in the high magnetic field ($g < 2$) region, but a new intense signal was observed in the low field region near $g = 16$ (25). Mössbauer spectroscopy showed that all of the iron was present as high spin Fe(II) ($S = 2$), which is normally EPR silent. We subsequently showed that the $g = 16$ signal arose from the ferromagnetically coupled, fully reduced diiron cluster $\{[\text{Fe(II)}\bullet\text{Fe(II)}]\}$ that exhibits an integer electronic spin ($S = 4$) (33). EPR signals from integer spin states are rare, and that from fully reduced MMOH represents one of the best examples known. The $g = 16$ signal of MMO has been a useful spectroscopic probe of the diferrous state of the cluster, which as shown in experiments described below, is the form of the enzyme that reacts with O_2 .

Diiron clusters similar to the type found in MMOH are present in several important proteins and enzymes, including mammalian ribonucleotide reductase (50, 54), hemerythrin (62), fatty acid desaturases (24), and purple acid phosphatases (12) such as uteroferrin (3). However, because none of these

proteins have oxygenase activity in their native state, determining whether the site of oxygenase activity was actually located on the MMOH component became important. Indeed, the flavin found in the reductase component is a common oxygenase cofactor and represents a reasonable alternative active site. The localization of the active site was accomplished by conducting single turnover experiments in which each homogeneous component in the absence of the other components was stoichiometrically reduced by nonenzymatic reductants (19). Upon exposure to methane and O₂, each component reoxidized. Only the MMOH component catalyzed methane oxidation during the reoxidation process, showing definitively that this component with its diiron cluster was responsible for catalysis. Moreover, only the fully reduced state of the cluster supported turnover, showing that this is the state from which catalysis must ensue. This experiment greatly simplified the consideration of MMO catalysis and provided a starting point for the studies of the mechanism described below.

ADVANCED STUDIES Although the preliminary spectroscopic studies showed that the diiron clusters of MMOH and other proteins were similar, the unique oxygenase activity of MMOH clearly indicated important differences. Consequently, more detailed spectroscopic studies were undertaken to better characterize the cluster structure. Hodgson and coworkers (15, 17) used X-ray absorption spectroscopy, in particular extended X-ray absorption spectroscopy fine structure (EXAFS), to show that the cluster irons are 3.42 Å apart. Moreover, the iron ligation was similar to that of inorganic model complexes in which the irons are bridged by one or two carboxylates in addition to the oxygen bridge. However, no short-bond characteristic of an oxo-bridging ligand was observed, leading to the suggestion that the oxygen bridge in MMOH is protonated or otherwise substituted. A similar conclusion was reached from analysis of the Mössbauer spectra of samples measured at temperatures above 50 K (21, 25).

MMOH has now been extensively studied using the Mössbauer technique (46) in each of the three redox states that have been discussed thus far (21, 25). In addition, recent developments have allowed Mössbauer characterization of a probable [Fe(IV)•Fe(IV)] form of MMOH (discussed below) (37). The spectra showed that the irons are in slightly different environments (21), and this difference has been combined with information from X-ray crystal diffraction data (29) to show that there must be two clusters in the *M. trichosporium* enzyme in contrast to the single cluster reported for the *M. capsulatus* enzyme (11, 17, 67).

The use of electron nuclear double resonance (ENDOR) has shown that at least nine different protons reside within a few Ångströms of the mixed valence MMOH diiron cluster (32). Three of these protons exchanged with D₂O slowly

over an 8-h incubation. The superhyperfine coupling constants (A values) of these exchangeable protons are appropriate for histidine ligation, as confirmed through the observation of ^{14}N ENDOR (32) resonances from histidines associated with both the Fe(II) and Fe(III) of the mixed valence cluster. Two proton resonances were observed at $A_{\text{H}} = 8$ and 13 MHz that were too strongly coupled to be assigned to amino acid ligands. They could not be further assigned because no proton exchange was noted after 8 h of incubation in D_2O . Recent research has shown that the protons giving rise to both of these resonances exchange with D_2O after 24 h of incubation. Comparison of these ENDOR resonances with those of hemerythrin showed that the $A_{\text{H}} = 8$ MHz proton was associated with a terminal hydroxide ligand on one of the irons, whereas the $A_{\text{H}} = 13$ MHz proton was associated with the bridging oxygen (14, 63). This means that the oxygen bridge in mixed valence MMOH is protonated in accord with the EXAFS and Mössbauer results cited above.

Magnetic circular dichroism (MCD) (60) of diferrous MMOH and the diferrous MMOH-component B complex showed that, in each case, both the irons of the diiron cluster had five ligands arranged in distorted square pyramidal coordination geometries (57). However, the addition of component B significantly perturbed the spectrum, suggesting that a structural change in the active-site region occurs. Other evidence for such a change is presented below.

Resonance Raman spectroscopy has been a very useful technique in the study of other proteins containing diiron clusters because these proteins all have visible chromophores. Unfortunately, this is not true for MMOH. However, we found that when phenol or a substituted phenol was added to the MMOH, a red or brown chromophore slowly appeared (1). Resonance Raman spectra of these MMOH complexes showed bands in a region indicative of a charge transfer interaction as the origin of the visible chromophore. Thus, the phenol binds directly to the iron as a phenolate. This was the first direct demonstration that large molecules could bind to the cluster, suggesting that it is somewhat accessible to exogenous ligands.

STRUCTURE OF THE ACTIVE SITE These spectroscopic studies can be combined to yield the view of the MMOH diiron cluster shown in Figure 2. Investigators tentatively identified the specific amino acid ligands by comparing the gene sequence of the MMOH α subunit with a homologous region of the primary sequence of the R2 subunit of ribonucleotide reductase (7, 49, 50). The crystal structure of R2 shows that this region contains the diiron cluster (50). The basic features of this alignment, such as the presence of one histidine in the coordination of each iron, are confirmed by the spectroscopic studies. However, features such as the accessibility of the MMOH cluster and the coordination number and geometry are different from those of R2. These structural

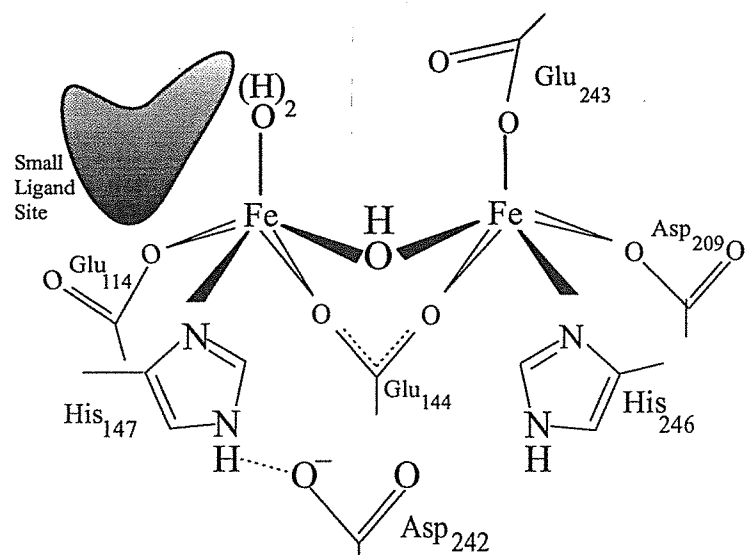


Figure 2 Hypothetical structure of the active-site, oxygen-bridged diiron cluster of MMOH. The structure shown here represents a compilation of the conclusions drawn from spectroscopic studies as described in the text (1, 15, 17, 21, 25, 32, 33, 68). The bridging OH ligand and histidine ligation have only been established for the mixed valence state (14, 63). The five-coordinate iron ligation has only been established for the diferrous state (57). The specific amino acid assignments are based on sequence alignment of the α subunit with ribonucleotide reductase subunit R2 (7, 49, 50). All of the features of this structure were recently confirmed by the X-ray crystal structure of MMOH isolated from *M. capsulatus* (Bath) (58a).

features may play important roles in determining the catalytic role of the diiron cluster.

MECHANISM

Two observations influenced the development of a hypothesis for the mechanism of MMOH. First, the single turnover experiment (19) described above showed that the diferrous state of the MMOH reacts with O_2 in the catalytic cycle. Second, many of the reactions catalyzed by MMOH were the same as (or analogous to) those catalyzed by P-450. Investigators generally agree (44) that the mechanism of P-450 centers around generation of a highly reactive porphyrin π cation radical $Fe(IV)=O$ (oxene) species as the direct oxidant of unactivated hydrocarbons. This species is chemically reasonable but has never been directly observed.

The proposed mechanism for MMOH (Figure 3) encompasses the diferrous

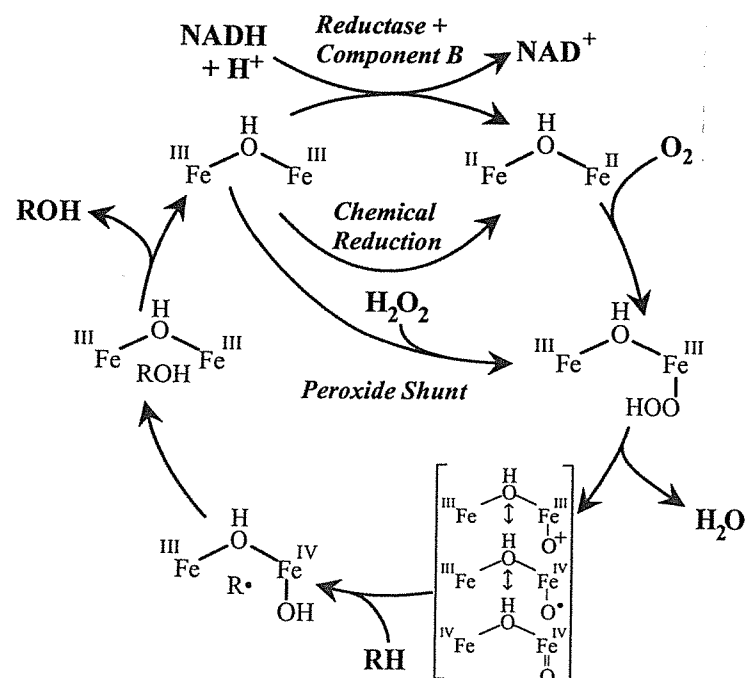


Figure 3 Proposed reaction cycle for MMO. MMOH is illustrated only as the active-site diiron cluster. A number of studies led to this proposed mechanism (18, 19, 25, 44), and several reports have supported it (2, 13, 27, 30, 37, 38, 56, 58, 59).

state of the cluster and mimics the mechanism of P-450 (2, 18, 19, 27, 28). Here, O_2 binds to one or both irons of the diferrous cluster, leading to heterolytic O-O bond cleavage to release water. The remaining oxygen atom (six valence electrons) remains bound to the formally $[\text{Fe(III)}\bullet\text{Fe(III)}]$ cluster. The most stable resonance form of this complex would be achieved by transfer of one electron from each of the irons to the oxygen to complete its valence shell. This $[\text{Fe(IV)}\bullet\text{Fe(IV)}]=\text{O}$ species of MMOH is equivalent to the oxene species of P-450; such a species would be a powerful oxidizing reagent of the type required to attack methane. This oxidant may abstract a hydrogen atom from the substrate to form a substrate radical and the iron-bound equivalent of a hydroxyl radical. Radical recombination, or rebound, would yield the product alcohol and recycle the enzyme to the diferric state.

This mechanism is attractive because it postulates the generation of the only type of reagent known to attack unactivated hydrocarbons in biology, a metal-bound oxene. Moreover, it provides a rationale for nature's selection of the

diiron cluster, because this cluster can both store the two electrons required to initiate catalysis and provide the two electrons required to stabilize formation of the reactive intermediate. Both chemical and kinetic approaches have produced evidence supporting this mechanism.

Chemical Approaches

PEROXIDE SHUNT CHEMISTRY One can view the mechanism shown in Figure 3 as an activation phase followed by a reaction phase in which the actual chemistry of hydrocarbon oxidation occurs. In the activation phase, the metal-bound oxene is generated by the addition of two reducing equivalents and O_2 to the MMOH. In principle, the two reducing equivalents and O_2 could be added together in the form of H_2O_2 . Thus, the mechanism predicts that diferric MMOH could catalyze hydrocarbon oxidation anaerobically and without NADH, reductase, and component B if H_2O_2 were present. This supposition proved to be correct (2, 27) and is illustrated as the peroxide shunt in Figure 3. Representative hydrocarbons from all of the classes of MMO substrates react via the peroxide shunt to yield the same products as the fully reconstituted system. Continuous turnover was observed with little loss in activity in 10 mM H_2O_2 for 30 min; thus the enzyme is resistant to damage by peroxide. Organic peroxides such as cumene hydroperoxide and single oxygen atom transfer reagents such as periodate did not support turnover. Similar peroxide shunt chemistry has been observed for P-450 (35). This enzyme was damaged by peroxides after only a few turnovers, but a wide range of organic peroxides and single oxygen-atom transfer reagents could substitute for H_2O_2 .

SUBSTITUENT MIGRATION Both P-450 and MMO catalyze substituent migration reactions as a result of the formation of transient carbocation intermediates. One type of group migration reaction was observed when P-450 (45) or MMO was supplied with 1,1,2-trichloroethylene (TCE) or other halogenated ethylenes (18). The predominant product in all cases was a semistable epoxide that spontaneously hydrolyzed after release from the enzyme, breaking down into a variety of dehalogenated products. Because TCE and similar potentially carcinogenic solvents of human manufacture persist in the environment in enormous quantities, this reaction of MMO is currently receiving substantial attention (64). However, the mechanistically most significant reaction of MMO with TCE was a minor formation of 2,2,2-trichloroacetaldehyde (chloral) in which a chlorine substituent had migrated to the adjacent carbon. This reaction did not occur with synthetic TCE epoxide in solution, so it must have occurred during the reaction in the active site. The most reasonable mechanism involves electron abstraction from the ethylene double bond π system to form an intermediate substrate radical. Rebound of the oxygen to one carbon would

yield a cation on the other, which could be quenched by migration of the metal-oxygen bond to form an epoxide, or by migration of a chlorine to form the aldehyde. In either case, the occurrence of cationic character implied by substituent migration is consistent with the formation of a very electron-deficient reagent in the active site of the type we have proposed.

SUBSTRATE INTERMEDIATE EPIMERIZATION Perhaps the most diagnostic feature of the proposed mechanism shown in Figure 3 is the transient formation of a substrate radical. Such a species could only be formed by an exceptionally powerful oxidizing reagent like the diiron cluster-bound oxene. Many approaches have been used to search for evidence for the intermediate substrate radical. One of the most definitive experiments was carried out by Donnelly and coworkers (58) who showed that the MMO-catalyzed oxidation of *exo, exo, exo, exo* d₄-norbornane resulted in the formation of some of the d₄ *exo* alcohol. This observation implied that an intermediate, probably a radical, formed that could epimerize before oxygen rebound. Several years ago, Groves and coworkers (31) showed that P-450 could catalyze this reaction in the same way. Other diagnostic rearrangements such as allylic migration are catalyzed by MMO from both type X and type II methanotrophs (30, 58).

RADICAL CLOCK CHEMISTRY Another approach to this problem is to use a so-called radical clock reagent, which generally contains a strained cyclopropane ring. A radical formed on a substituent of the ring will migrate to the ring and cause it to open at a characteristic rate. Frey and coworkers (59) showed that MMO-catalyzed oxidation of 1,1-dimethylcyclopropane undergoes ring opening about 6% of the time, consistent with radical formation. However, many other products were formed including 1-methylcyclobutanol, a product indicative of formation of a cationic intermediate. For a saturated substrate like 1,1-dimethylcyclopropane, formation of a cation would require that two electrons or hydrogen atoms be withdrawn.

The studies of Lippard and coworkers (41) lead to a different conclusion for the *M. capsulatus* MMO. In these studies, a set of radical clocks were used that rearrange very rapidly (as fast as 5% of a typical bond vibration rate). Nevertheless, no rearrangement was observed within experimental error, suggesting that an intermediate radical was not formed. In contrast, when the *M. trichosporium* enzyme was used, a small amount of ring opening (~3% of total) was observed. Thus, it was proposed that the two enzymes may have somewhat different mechanisms.

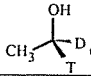
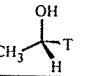
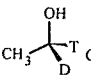
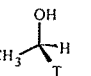
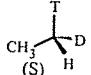
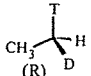
INVERSION OF CHIRAL SUBSTRATES The approaches described above are based on the oxidation of diagnostic molecules that are unlike methane in both structure and bond energy. Accordingly, many products result from catalysis.

To the extent that these products indicate radical intermediates, they support the mechanism shown in Figure 3. However, the fact that other products are formed means that these approaches can only show that substrate radical formation is one mechanism of MMO, not that it is the only mechanism for methane turnover.

The size and shape of the diagnostic molecules can have a large impact on the interpretation of results (41). In order to avoid such uncertainties, we approached the problem by selecting the substrate most like methane that could be made chiral, namely ethane (56). The stereospecific placement of deuterium and tritium on one of the carbons results in chiral ethane. When MMO catalyzes the conversion of this molecule to ethanol, the product will either retain the same chirality, or it will be inverted. Complete retention or complete inversion of chirality would indicate a reaction mechanism in which no free intermediate was generated. In contrast, partial inversion would show definitively that an intermediate free to rotate in the active site occurred during the reaction. The use of chiral ethane also allows the stereochemical configuration of the products to be directly evaluated using $^3\text{H-NMR}$ if carrier-free chiral ethane is used as the substrate. The experiment carried out with R or S chiral ethane showed approximately 35% inversion of configuration (Table 1) (56). Thus, the reaction involves a free intermediate, which is probably an ethyl radical because the alternative, a free ethyl cation, has never been generated chemically at neutral pH.

The fact that the extent of inversion is only 35% implies, first, that the reaction must occur completely within the active site because a radical diffusing outside the active site would be quenched completely randomly and show 50% inversion. Second, the rebound reaction must be very fast because the rotation of the ethyl radical probably occurs around the single C-C bond with a rate of between 10^{12} and 10^{13} s^{-1} . The intramolecular deuterium isotope effect

Table 1 Product distribution from oxidation of chiral ethane by MMO.^a

Substrate Ethane	Distribution of Stereoisomers (%)			
				
 (S)	27 (36 % Inversion)	7	52 (64 % Retention)	14
 (R)	53 (68 % Retention)	12	26 (32% Inversion)	9

^a Data from reference (56). Reconstituted MMO system coupled to NADH oxidation.

for the reaction was 4.2 at 25°C. This value is consistent with complete C-H bond breaking in the transition state.

The chiral ethane experiment offers the strongest evidence that the reaction proceeds via a radical substrate intermediate as proposed in Figure 3. A similar conclusion was reached by Dalton and coworkers using radical trap reagents (13).

Transient Kinetic Approaches

The use of transient kinetic techniques to directly detect intermediates in the reaction cycle and measure their rates of interconversion represents a powerful means of characterizing the mechanism of an enzyme. If one of the goals of the study is to determine rate constants for the formation and decay of the intermediates, the overall reaction must be established with a definite starting and ending point. In the case of MMOH, this is accomplished by beginning the reaction with the MMOH stoichiometrically reduced to the diferrrous state, as illustrated in Figure 4. Upon addition of O₂ and substrate, the enzyme will undergo a single turnover and stop at the diferric state. To date, only the transient kinetics of the MMOH– component B complex in the presence and absence of substrate have been investigated (38).

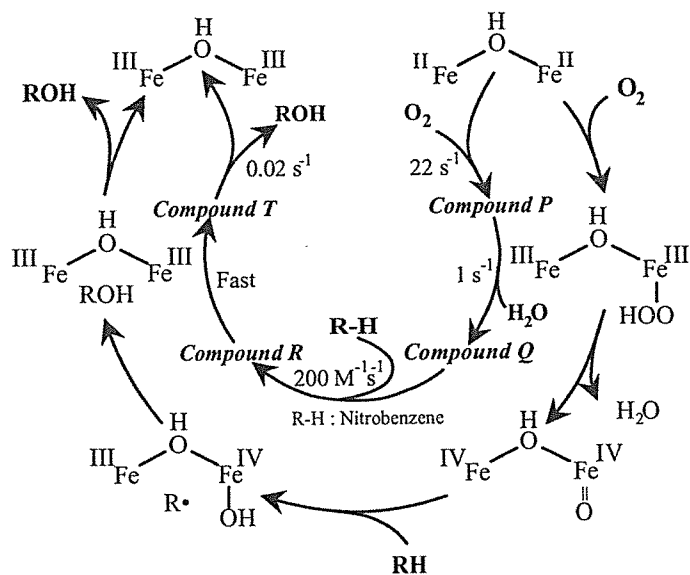


Figure 4 Single turnover cycle of MMOH and rate constants for interconversion of intermediates (37, 38). (Outer circle) Proposed mechanism for a single turnover of diferrrous MMOH. (Inner circle) Rate constants determined for the interconversion of the observed intermediates during a single turnover with 1 mM nitrobenzene present as a substrate (RH). All measurements were made using solutions at 4°C.

FREEZE QUENCH STUDIES The diferrous state of MMOH is colorless, so the convenient optical detection techniques often used in transient kinetic studies could not be employed. Instead, samples were mixed with O₂ at 4°C in a rapid-flow mixing device and then rapidly frozen after precise delay intervals by ejecting them through a spray nozzle into a -140°C isopentane bath. The frozen samples could then be studied with EPR spectroscopy to monitor the loss of the $g = 16$ signal characteristic of the diferrous state. This reaction occurred very rapidly with an apparent first-order rate constant of $\sim 22 \text{ s}^{-1}$ (38). This rate is about 50 times the turnover number of the reconstituted MMO system for methane at 4°C.

STOPPED FLOW STUDIES Although diferrous MMOH is colorless, it briefly turns yellow after exposure to oxygen (38). We investigated this observation using optically monitored stopped flow techniques. The rapid scan stopped flow technique was used to record full spectra of the yellow intermediate, which we have named compound Q. In the absence of substrate, the intermediate formed and decayed with rate constants of about 1.0 s^{-1} and 0.05 s^{-1} , respectively, as illustrated in Figure 5. It exhibited absorbance maxima at 330 and 430 nm with the same extinction coefficient at each wavelength, $\epsilon = \sim 7500 \text{ M}^{-1} \text{ cm}^{-1}$. This is a unique species unlike any previously described in transient kinetic studies of other proteins, enzymes, or model compounds containing diiron clusters (6, 39, 40).

The rate constant measured for the decay of diferrous MMOH is about 20-fold faster than the formation of compound Q. Therefore, at least one, and possibly several, intermediates must form and decay in the time between O₂ binding and compound Q formation. We have designated compound P as the immediate precursor of compound Q. The existence of compound P is also suggested by the fact that the formation rate of compound Q is independent of O₂ concentration. Thus, an irreversible step must occur between O₂ addition and compound Q formation. The spectroscopic characterization of compound P is currently in progress.

The addition of substrates caused little or no change in the formation rate of compound Q, but the decay rate increased dramatically (38). Significantly, the decay-rate constant increased linearly with the substrate concentration at pH 7.7, suggesting that compound Q reacts directly with substrate in what appears kinetically as a collisional reaction. The reaction may, in fact, be a binding reaction followed by a fast chemical reaction; this would show the same apparent kinetics. The type of substrate used was found to greatly affect the apparent second-order rate constant for the decay reaction. Thus, the rate constant for the reaction with methane is 45 times that for the reaction with nitrobenzene, in rough accord with the turnover numbers for these substrates.

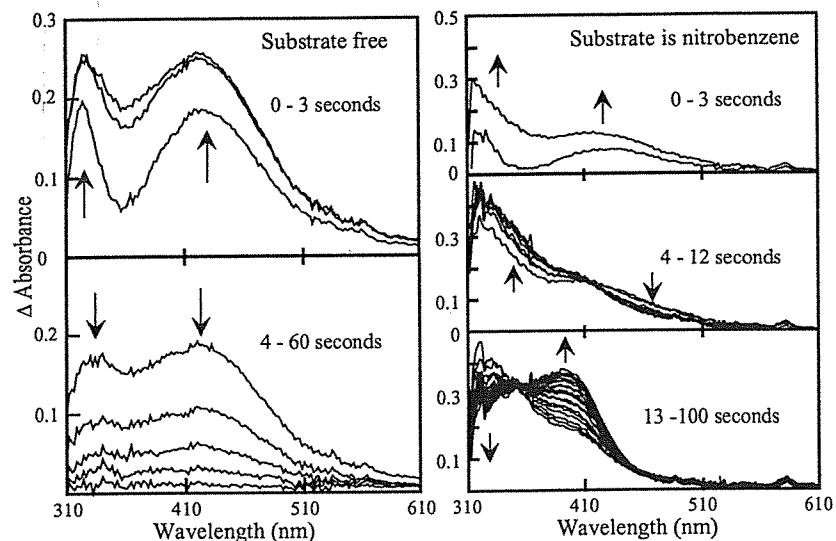


Figure 5 Formation and decay of chromophoric intermediates in the MMOH reaction cycle (38). (Left) Formation (top) and decay (bottom) of compound Q in the absence of substrate. Diferrous MMOH was rapidly mixed with saturated O_2 solution at $4^\circ C$. The spectra showing the formation and decay of compound Q were followed over the next 60 s using a diode array rapid scan device. (Right) The experiment was repeated with the addition of nitrobenzene (substrate) to the O_2 solution before mixing. The decay of compound Q is more rapid and passes through compound T as shown in the middle panel. Reprinted with permission from Ref. 38.

Nitrobenzene oxidation provided another means of following the kinetics of turnover because one of the major reaction products is *p*-nitrophenol, which has a strong chromophore at 404 nm. Rapid scan stopped flow spectroscopy showed that this product was not formed directly from compound Q. Rather, an intermediate formed at a rate constant of $200 M^{-1} s^{-1}$ ($0.2 s^{-1}$ pseudo first-order rate constant at 1 mM nitrobenzene) with an absorption maximum at 325 nm and an isosbestic point at 415 nm. Subsequently, the intermediate, which we have termed compound T, decayed with a different isosbestic point (at 350 nm) to form the final species exhibiting the optical spectrum of *p*-nitrophenol. The rate constant for this final decay was $\sim 0.02 s^{-1}$, about the same as the turnover number for nitrobenzene in the reconstituted, NADH-coupled MMO system at $4^\circ C$. This suggests that the product release step is rate limiting in the overall catalytic cycle of MMO.

CHEMICAL QUENCH STUDIES Compound T was proposed to be an enzyme-*p*-nitrophenol (product) complex on the basis of the similarity of its optical spectrum to that of *p*-nitrophenol dissolved in nonpolar solvents. Evidence

supporting this proposal came from studies in which the reaction was quenched, at precise intervals during the decay of compound Q, by ejection of the reaction mixture through a spray nozzle into room-temperature chloroform (38). The solvent denatures the enzyme and releases any product residing in the active site. This method allows one to ascertain the true rate of product formation independent of its release rate. The results showed that *p*-nitrophenol was formed at about the same rate as compound Q decay and compound T formation. Because this is more than 10-fold faster than product release at the substrate concentrations used, compound T is clearly the enzyme-product complex.

CHEMICAL NATURE OF COMPOUND Q The inner circle of Figure 4 summarizes the rates of the single turnover reaction of nitrobenzene. Clearly, the rates of interconversion decrease progressively throughout the cycle, which is the ideal kinetic circumstance for trapping and characterizing each intermediate. These studies are now in progress, and the first intermediate trapped by using the freeze-quench technique was compound Q (37). The MMOH used for the experiment was enriched with ^{57}Fe so that the nature of compound Q could be evaluated with Mössbauer spectroscopy. After subtraction of the known spectra of the unreacted diferrous MMOH and product diferric MMOH, the spectrum of compound Q became evident (Figure 6). The spectrum consists of a quadrupole doublet with parameters indicative of intermediate or high spin Fe(IV). Moreover, all of the iron in compound Q is Fe(IV) because only one doublet is observed. The spectrum of the sample in a high magnetic field showed that compound Q is diamagnetic. Because Fe(IV) would be paramagnetic in biological systems, the diiron cluster must persist in compound Q and the irons must be strongly antiferromagnetically coupled. This is the first Fe(IV) cluster to be observed in biology.

Several observations suggest that compound Q is the activated oxy species that attacks hydrocarbons: (a) it forms after the addition of O_2 to the diferrous MMOH, but before product is released, so it contains oxygen from O_2 ; (b) its formation rate is generally independent of substrate concentration; (c) its decay reaction appears to involve direct collision with substrate; and (d) it yields product at the same rate as its decay. Thus the $[\text{Fe(IV)}\bullet\text{Fe(IV)}]$ -oxene species present in compound Q appears to be the first intermediate capable of unactivated hydrocarbon oxidation to be trapped for any heme or nonheme oxygenase, including P-450.

Given the similarity in number and chemical characteristics of the intermediate compounds described for MMOH turnover to those of the hypothetical mechanism, the tentative assignments shown in the outer circle of Figure 4 are reasonable. However, the detailed structure of the compounds cannot yet be

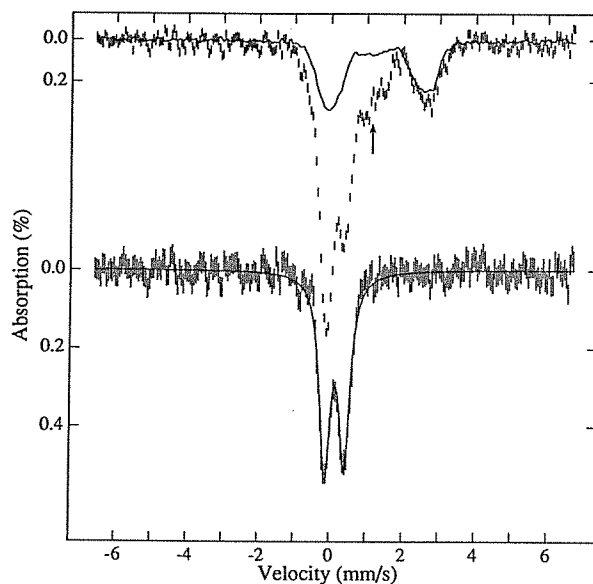


Figure 6 Mössbauer spectrum of compound Q (37). (*Top*) Diferrous ^{57}Fe -enriched MMOH was rapidly mixed with saturated O_2 and frozen by rapid freezing techniques after 4 s. Mössbauer spectra were recorded for a sample at 4 K. The solid line is the spectrum of diferrous MMOH frozen after rapid mixing with anaerobic buffer. The arrow marks one of the spectral lines of diferric MMOH present in the sample as the end product of compound Q decay. (*Bottom*) Spectrum of compound Q obtained by subtraction of the spectra of diferrous (30%) and diferric (25%) MMOH present in the sample. All samples contain component B (2:1 versus MMOH sites). Reprinted with permission from Ref. 37.

determined. For example, the Mössbauer spectrum of compound Q (Figure 6) reveals only one sharp quadrupole doublet, showing that the two irons are in essentially identical electronic environments. This would not be the case if the oxene were associated with only one iron as depicted in Figures 3 and 4. Instead, the activated oxygen species must be symmetrically bound by the two irons. Figure 7 shows some possibilities for this structure, but we cannot yet choose the correct structure given the data at hand.

THE ROLES OF REDUCTASE AND COMPONENT B IN THE CATALYTIC CYCLE

Although the catalytic studies summarized above indicate that the reductase and component B are not required for turnover, these components do have substantial effects on the rate and specificity of turnover under certain circum-

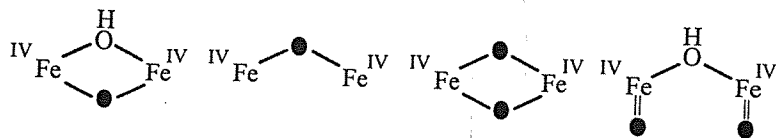


Figure 7 Possible symmetrical structures for the diiron cluster of compound Q. Water formally derived from O_2 (filled circle) has dissociated from the cluster for the two structures on the left, but not for the two on the right.

stances. These effects appear to be mediated by the formation of stable complexes between the components (23). The impact of these complexes on regulation of the catalytic cycle is now beginning to emerge.

One of the most powerful tools in the study of the roles of the reductase and component B has been the discovery of the three catalytically functional subsystems of MMO (27): (a) system I—NADH, reductase, MMOH, O_2 ; (b) system II—diferric MMOH, H_2O_2 ; (c) system III—diferrous MMOH, O_2 .

Each of these requires MMOH but not component B. Systems II and III also do not require the reductase. They all give the same products as the fully reconstituted system for all classes of MMO substrates. Systems I and II are catalytic, turning over indefinitely, whereas system III turns over only once. We have used these systems to determine the effects of adding reductase and/or component B under a variety of conditions.

Complex Formation

STEADY-STATE KINETICS For system I with reductase and MMOH in equimolar (sites) concentration, the addition of component B caused the initial velocity to increase sharply (Figure 8). At the point where the component B concentration roughly matched the MMOH active-site concentration, the initial velocity maximized (23). It then gradually decreased with additional component B. When the reductase to MMOH ratio was increased, the maximal rate increased to a higher saturable maximum and more component B was required to reach this maximum. These kinetic phenomena can be accounted for by assuming that: (a) a ternary complex of one reductase and one component B per active site of MMOH is required for the most efficient NADH catalysis; (b) an inhibitory complex forms in which a second component B binds per MMOH active site; and (c) reductase forms a complex with component B that removes component B from the equilibrium with MMOH. Under these assumptions, the kinetic data can be fit with the set of K_d values shown in Figure 8, which indicate very strong affinity between the components.

CHEMICAL CROSSLINKING AND FLUORESCENCE STUDIES High affinity complexes can often be directly detected using chemical and spectroscopic tech-

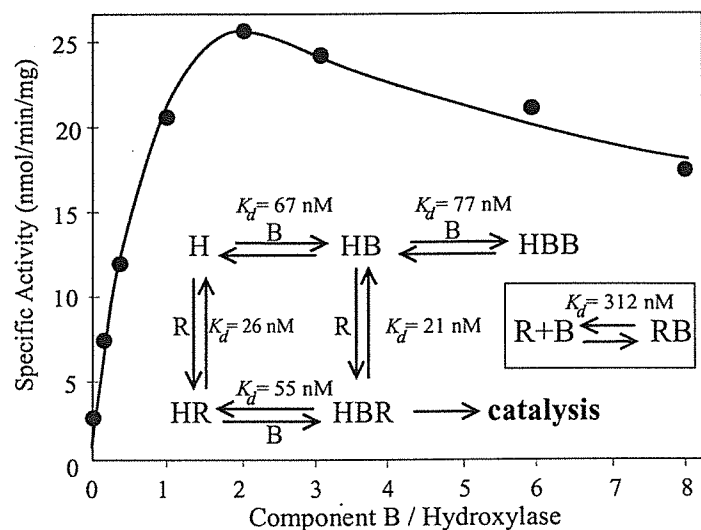


Figure 8 Effect of component B on the initial velocity of MMO turnover. The data show the activating and inactivating effects of component B for a 1:1 ratio of reductase and MMOH active sites. The solid line is a fit based on the scheme and equilibrium constants shown. The HBB and RB complexes are assumed to be inhibitory and only the HBR complex supports rapid turnover. H is the MMOH active site; R is the reductase; B is the component B. Data were recorded at room temperature (23, 27).

niques. All of the complexes indicated on Figure 8 were detected using chemical crosslinking and fluorescence spectroscopy (23). The reagent 1-ethyl-3-(3-dimethylaminopropyl)-carbodiimide (EDC) reacts to form a bond between protein amino and carboxyl groups that normally form salt linkages in a component complex. Specific crosslinks were formed for the component B and reductase with the α - and β -subunits of MMOH, respectively, indicating that each component has a specific binding site on MMOH. Interestingly, EDC also reacted very rapidly with component B alone to cause loss of its ability to stimulate the reconstituted system. Only a fraction of the EDC-treated component B formed crosslinked dimers, but rate-enhancement activity was completely lost. Hence, crosslinking of surface groups on individual component B molecules probably interferes with component B's ability to bind to MMOH, demonstrating the necessity of complex formation for rate enhancement.

Both MMOH and component B are fluorescent near 340 nm when irradiated at 280 nm because of one or more tryptophans in relatively polar environments (23). When a complex forms between MMOH and either of the other components, the fluorescence is quenched and blue shifted, allowing the K_d values

to be determined by direct titration. The stability of the component B-reductase complex was also measured in the same way. Remarkably, the actual dissociation constants agree well with those predicted by the fit to the steady-state model described above.

EPR STUDIES EPR spectroscopy provides a sensitive means of monitoring the effects of complex formation on the active site. The EPR signal from the mixed valence state changed dramatically when the complex between MMOH and component B was formed (23). The resonances were shifted to $g = 1.87, 1.77, 1.62$, and the magnitude of the exchange coupling constant describing the antiferromagnetic coupling of the irons (J) dropped sixfold from $\sim 30 \text{ cm}^{-1}$ to $\sim 5 \text{ cm}^{-1}$. Likewise, the $g = 16$ signal of the diferrous state became sharper and more intense upon binding of component B. These and similar observations from other spectroscopic studies indicate that the surface interaction of MMOH and component B causes structural changes that are transmitted to the diiron cluster. The formation of the MMOH-reductase complex did not cause dramatic spectral changes, but measurable changes in the J value of the mixed valence state were observed.

OXIDATION/REDUCTION POTENTIALS The two formal redox potential values for MMOH from *M. capsulatus* were determined in two independent studies (42, 43, 68), and we recently made analogous measurements for *M. trichosporium* MMOH (53). The two studies of the *M. capsulatus* MMOH utilized the same set of 12 indicator dyes to facilitate the establishment of equilibrium and provide a reliable measurement of the overall system potential by monitoring electrodes. In each study, the amount of mixed valence MMOH was quantitated by EPR spectroscopy and used to calculate the extent of reduction at a given system potential. Despite their similar protocols, the two studies gave quite different results. Dalton and coworkers (68) found values of $E_1^{\circ'} = +350 \text{ mV}$ and $E_2^{\circ'} = -25 \text{ mV}$, while Liu & Lippard (42, 43) found $E_1^{\circ'} = +48 \text{ mV}$ and $E_2^{\circ'} = -135 \text{ mV}$. The latter group reported that addition of reductase and component B to MMOH blocked electron transfer to the diiron cluster unless propylene, an alternate substrate, was also present.

Our study of the *M. trichosporium* MMOH (53) showed that two of the 12 dyes used in the earlier studies bind to MMOH and change its spectroscopic properties, perhaps explaining the widely varying results. Also, the determination of redox potentials in these studies depended on the accurate determination of the total cluster concentration and the amount of the cluster in each redox state during the titration. Measuring the necessary values with sufficient accuracy is difficult with EPR quantitation alone. In studying the *M. trichosporium* MMOH, we used Mössbauer spectroscopy to provide these values at several points in the titration. This technique allows accurate quan-

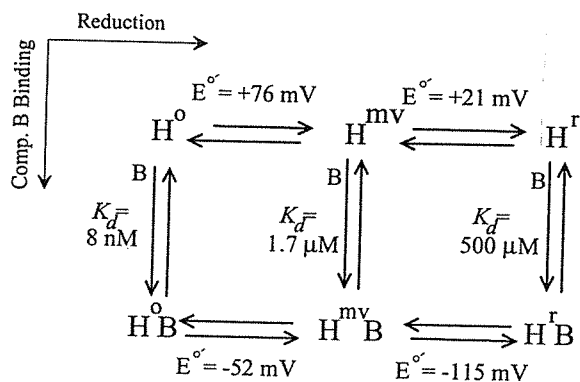


Figure 9 Thermodynamic-state diagram relating component B (B) binding and MMOH (H) redox potential. The K_d value for the formation of the diferric MMOH–component B complex was determined by fluorescence titration (see text). The K_d values for the mixed valence and diferrous MMOH complexes with component B were calculated from the measured redox potentials (53). Asymmetry in the cycle (unequal values on opposite sides of the figure) shows that the binding and redox reactions are coupled. Reprinted with permission from Ref. 53.

titration of each redox state simultaneously in a single sample. The *M. trichosporium* MMOH titration showed formal potentials of $E_1^{o'} = +76$ mV and $E_2^{o'} = +21$ mV (± 15 mV) ($E_{\text{mid}} = -48$ mV). Upon addition of component B (2:1 vs MMOH active sites), the MMOH potentials shifted negatively to $E_1^{o'} = -52$ mV and $E_2^{o'} = -115$ mV (± 15 mV) ($E_{\text{mid}} = -84$ mV).

As shown in Figure 9, one can construct a thermodynamic-state diagram using these changes in potential to predict the changes in affinity between the component B and MMOH when the MMOH is reduced (53). A decrease in affinity of between four and five orders of magnitude is expected. The affinity of the diferrous MMOH–component B complex was directly evaluated using a fluorescence titration. The affinity of this complex was more than three orders of magnitude less than that of the diferric MMOH–component B complex (Y Liu & JD Lipscomb, unpublished observation), in approximate agreement with the prediction from the potentiometric measurements.

In contrast to the results reported for the *M. capsulatus* MMO system, when reductase was added to the MMOH–component B complex, the redox potentials were similar to those of MMOH alone (53). Thus, the reductase can in some manner obviate the effect of component B on the redox potential of MMOH. Interestingly, the relative magnitudes of $E_1^{o'}$ and $E_2^{o'}$ for MMOH are reversed whenever reductase is bound to MMOH. This effect thermodynamically stabilizes the active diferrous MMOH.

The addition of substrates to the ternary MMO component complex also caused minor changes in potential relative to the complexes alone. However,

the several-hundred-millivolt increase in midpoint potential reported for the *M. capsulatus* enzyme (42, 43) upon addition of substrate to the complex of all three components was not observed for *M. trichosporium* MMOH.

Product Distribution Studies

The MMO mechanism shown in Figure 3 emphasizes the predominant role of the MMOH diiron cluster in catalysis. If the reductase and component B served only to facilitate transfer of electrons to MMOH, then these components would affect only system I. Moreover, only this system's rate of reduction would be altered. In particular, no effects on the product-forming portion of the reaction of any of the systems would be anticipated. Although the systems do in fact produce the same products, two observations show that the reductase and component B must have roles beyond electron transfer in catalysis (27). First, no electron transfer is required in system II, but component B causes the system to slow down by as much as 80% for most substrates. Second, the systems give very different product distributions for many substrates that can be oxidized at more than one carbon. Moreover, component B and reductase dramatically alter the observed distributions.

Table 2 summarizes the product distributions for isopentane turnover in each system and the effect of component B on these distributions. The reductase also affects the distributions when added to system II and system III, but the differences are less dramatic. The distributions shown in Table 2 for reactions carried out in the absence of component B are all different from each other and from the distribution expected for the reconstituted MMO system (system I plus component B). Upon addition of component B, the distributions of systems I and III became identical to each other and to that for the reconstituted system. In system II, component B also caused the product distribution to shift toward primary carbon hydroxylation, but the distribution was still different from those of the other systems. Because the oxidants generated in the active site of MMOH in the three systems are unlikely to be different,² the distribution changes are probably related to the structural changes in MMOH caused by reduction of the cluster and/or binding of the components. The diiron cluster must assume the diferrous state during the reactions of systems I and III, but not during that of system II.

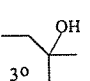
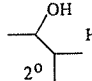
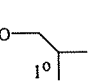
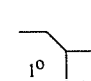
The results discussed above show that the structure of MMOH is altered by both the redox state of the diiron cluster and the thermodynamically coupled binding of component B (and reductase). Thus, the differences in product distribution could be ascribed to differences in the way a substrate can physi-

²All of the systems can turn over methane. Also, the percent inversion of chiral ethane is the same in systems I and II, implying that the same transition state occurs (WA Froland, JD Lipscomb, ND Priestley, HG Floss, PG Williams & H Morimoto, unpublished observation).

cally approach the activated oxygen in the active site of MMOH. This implies that the structure of the activated MMOH at the point of oxygen insertion has some memory of the system that produced it. That is, at least some of the systems must have hysteresis in the structural changes that is long relative to catalysis.

One can also examine the effects of the putative MMOH structural hysteresis by comparing the dependence of product distribution on component B concentration, as shown in Table 2. For systems I and III, the shift in product distribution was complete for component B at ~5% of the MMOH active-site concentration. In contrast, the initial velocity of turnover for system I was maximized at stoichiometric or greater concentrations of component B. Thus, component B clearly has two different effects on this system, implying that it has at least two roles in catalysis. In system II, the effects on both product distribution and initial velocity maximized at stoichiometric amounts of component B. One could explain the differences in the concentration dependence of the product distributions on component B in several ways, but most of these explanations require the assumption of rate enhancement in the MMOH–component B complex. Consequently, these can be discounted because system III is a single turnover system in which rate enhancement cannot amplify a particular product distribution. However, hysteresis in the relaxation of the component B–induced conformational change in MMOH would allow the entire population of MMOH to adopt an altered structure with only a small amount of component B present. This proposal requires that component B be

Table 2 MMO Catalyzed oxidation of isopentane

System ^a	B:H ^b Ratio	Product Distribution (%) ^c			
					
I and (III)	0	27 (38) ^d	30 (26)	30 (22)	13 (14)
	0.1	13 (13)	10 (7)	47 (49)	30 (31)
	1.0	11 (12)	8 (8)	51 (53)	30 (27)
	2.0	11 (11)	9 (7)	49 (52)	31 (30)
II	0	43	24	12	21
	0.1	42	23	13	22
	0.5	34	20	20	26
	1.0	26	19	29	26
	2.0	26	20	25	29
	8.0	26	19	28	27

^a See text for definition of catalytic systems.

^b Ratio of component B to MMOH (mol/mol)

^c Data from reference (27)

^d System III plus added reduced reductase gives a distribution indistinguishable from that of System I (which also contains reduced reductase).

able to dissociate rapidly from MMOH, which is apparently only possible for the diferrous MMOH due to its greatly reduced affinity for component B. In system II, where the MMOH remains oxidized with a high affinity for component B, a stoichiometric amount of component B is required to observe product-distribution changes.

Hysteresis in the structural changes of MMOH is supported by comparison of the EPR spectra of the mixed valent and diferrous MMOH in the presence of component B (27). For the mixed valence state, the EPR spectrum was altered progressively by formation of the MMOH-component B complex, maximizing the spectrum at equal active-site concentrations. In contrast, for the diferrous MMOH, the complete change in the $g = 16$ EPR signal lineshape was observed after addition of approximately 0.3 component B molecules per MMOH active site, indicating that an altered active-site conformation persists after component B dissociates for a period at least comparable to the freezing time of the sample.

Hypothesis for Regulation

Methane is the only physiologically relevant substrate of MMO. Thus, the structural changes in MMOH proposed to occur upon reduction of the diiron cluster and/or component complex formation are not designed to shift product distribution in vivo. Nevertheless, both reduction and component-component interactions are integral parts of the catalytic cycle of MMO. Therefore, the conformational changes in MMOH that occur in response to these events probably also occur during catalysis by the reconstituted enzyme system and are likely to play a specific role, one perhaps related to regulation of the catalytic cycle.

Figure 10 shows a hypothesis for the regulatory cycle of MMO. Resting MMOH will primarily form a complex with component B in vivo because the components are present in approximately equal concentrations and have high affinity. Reductase is present in the cell in only about 10% of the MMOH concentration, but its low K_d value for MMOH suggests that it will also be bound in the complex. Reduction of MMOH by the reductase would initiate catalysis. The reduced MMOH would have an inherently lower affinity for the component B. However, this would not be expressed until the reductase dissociates, because the redox potential of MMOH is coupled to the component B affinity. The redox potential and component B affinity will remain high as long as the reductase is bound. This part of the cycle assures that two electrons are irreversibly delivered to the MMOH before O_2 activation commences. Upon dissociation of the reductase, the redox potential of MMOH would drop, allowing O_2 to bind with high affinity and electron density to be delocalized into the O-O bond to facilitate its cleavage, with the consequent formation of compound Q. The associated increase in the K_d for component B would allow

collaborations with Professors Eckard Münck and Lawrence Que, Jr., which have contributed very significantly to the progress of these studies.

Any Annual Review chapter, as well as any article cited in an Annual Review chapter, may be purchased from the Annual Reviews Preprints and Reprints service. 1-800-347-8007; 415-259-5017; email: arpr@class.org

Literature Cited

1. Andersson KK, Elgren TE, Que L Jr, Lipscomb JD. 1992. Accessibility to the active site of methane monooxygenase: the first demonstration of exogenous ligand binding to the diiron cluster. *J. Am. Chem. Soc.* 114:8711-13
2. Andersson KK, Froland WA, Lee S-K, Lipscomb JD. 1991. Dioxygen independent oxygenation of hydrocarbons by methane monooxygenase hydroxylase component. *New J. Chem.* 15:411-15
3. Antanaitis BC, Aisen P, Lilienthal HR. 1983. Physical characterization of two-iron uteroferrin: evidence for a spin-coupled binuclear iron cluster. *J. Biol. Chem.* 258:3166-72
4. Anthony C. 1982. *The Biochemistry of the Methylootrophs*. London: Academic
5. Atwood MM. 1990. Formaldehyde dehydrogenases from methylotrophs. *Methods Enzymol.* 188:315-30
6. Bollinger JM Jr, Edmondson DE, Huynh BH, Filley J, Norton JR, Stubbe J. 1991. Mechanism of assembly of the tyrosyl radical-dinuclear iron cluster cofactor of ribonucleotide reductase. *Science* 253:292-98
7. Cardy DLN, Laidler V, Salmond GPC, Murrell JC. 1991. Molecular analysis of the methane monooxygenase MMO gene cluster of *Methylosinus trichosporium* OB3b. *Mol. Microbiol.* 5:335-42
8. Chan SI, Nguyen H-HT, Shiemke AK, Lidstrom ME. 1993. Biochemical and biophysical studies toward characterization of the membrane associated methane monooxygenase. See Ref. 46a, pp. 93-107
9. Colby J, Stirling DI, Dalton, H. 1977. The soluble methane monooxygenase of *Methylococcus capsulatus* Bath: its ability to oxygenate *n*-alkanes, *n*-alkenes, ethers, and alicyclic, aromatic and heterocyclic compounds. *Biochem. J.* 165:395-402
10. Dalton H. 1980. Oxidation of hydrocarbons by methane monooxygenases from a variety of microbes. *Adv. Appl. Microbiol.* 26:71-87
11. Dalton H. 1991. Structure and mechanism of action of the enzymes involved in methane oxidation. See Ref. 36a, pp. 55-68
12. Davis JC, Averill BA. 1982. Evidence for a spin-coupled binuclear iron unit at the active site of the purple acid phosphatase from beef spleen. *Proc. Natl. Acad. Sci. USA.* 79:4623-27
13. Deighton N, Podmore ID, Symons MCR, Wilkins PC, Dalton H. 1991. Substrate radical intermediates are involved in the soluble methane monooxygenase catalysed oxidations of methane, methanol and acetonitrile. *J. Chem. Soc. Chem. Commun.* pp. 1086-88
14. DeRose VJ, Liu KE, Kurtz DM, Hoffman BM, Lippard SJ. 1993. Proton ENDOR identification of bridging hydroxide ligands in mixed-valence diiron centers of proteins: methane monooxygenase and semimet azidohemerythrin. *J. Am. Chem. Soc.* 115:6440-41
15. DeWitt JG, Bentsen JG, Rosenzweig AC, Hedman B, Green J, et al. 1991. X-ray absorption, Mössbauer, and EPR studies of the dinuclear iron center in the hydroxylase component of methane monooxygenase. *J. Am. Chem. Soc.* 113:9219-35
16. Duine JA. 1991. Quinoproteins: enzymes containing the quinonoid cofactor pyrroloquinoline quinone, topaquinone or tryptophan-tryptophan quinone. *Eur. J. Biochem.* 200:271-84
17. Ericson A, Hedman B, Hodgson KO, Green J, Dalton H, et al. 1988. Structural characterization by EXAFS spectroscopy of the binuclear iron center in protein A of methane monooxygenase from *Methylococcus capsulatus* Bath. *J. Am. Chem. Soc.* 110:2330-32
18. Fox BG, Borneman JG, Wackett LP, Lipscomb JD. 1990. Haloalkene oxidation by the soluble methane monooxygenase from *Methylosinus trichosporium* OB3b: mechanistic and envi-

- ronmental implications. *Biochemistry* 29:6419-27
19. Fox BG, Froland WA, Dege J, Lipscomb JD. 1989. Methane monooxygenase from *Methylosinus trichosporium* OB3b: purification and properties of a three component system with high specific activity from a type II methanotroph. *J. Biol. Chem.* 264: 10023-33
 20. Fox BG, Froland WA, Jollie DR, Lipscomb JD. 1990. Methane monooxygenase from *Methylosinus trichosporium* OB3b. *Methods Enzymol.* 188: 191-202
 21. Fox BG, Hendrich MP, Surerus KK, Andersson KK, Froland WA, et al. 1993. Mössbauer, EPR, ENDOR studies of the hydroxylase and reductase components of methane monooxygenase from *Methylosinus trichosporium* OB3b. *J. Am. Chem. Soc.* 115:3688-3701
 22. Fox BG, Lipscomb JD. 1990. Methane monooxygenase: a novel catalyst for hydrocarbon oxidations. In *Biological Oxidation Systems*, ed. CC Reddy, GA Hamilton, MK Madyastha, pp. 367-88. San Diego: Academic
 23. Fox BG, Liu Y, Dege J, Lipscomb JD. 1991. Complex formation between the protein components of methane monooxygenase from *Methylosinus trichosporium* OB3b: identification of sites of component interaction. *J. Biol. Chem.* 266:540-50
 24. Fox BG, Shanklin J, Somerville C, Münck E. 1993. Stearoyl-acyl carrier protein Δ^9 desaturase from *Ricinus communis* is a diiron-oxo protein. *Proc. Natl. Acad. Sci. USA* 90:2486-90
 25. Fox BG, Surerus KK, Münck E, Lipscomb JD. 1988. Evidence for a μ -oxo bridged binuclear iron cluster in the hydroxylase component of methane monooxygenase: Mössbauer and EPR studies. *J. Biol. Chem.* 263:10553-56
 26. Froland WA, Andersson KK, Lee S-K, Liu Y, Lipscomb JD. 1991. Oxygenation by methane monooxygenase: oxygen activation and component interactions. See Ref. 36a, pp. 39-55
 27. Froland WA, Andersson KK, Lee S-K, Liu Y, Lipscomb JD. 1992. Methane monooxygenase component B and reductase alter the regioselectivity of the hydroxylase component-catalyzed reactions: a novel role for protein-protein interactions in an oxygenase mechanism. *J. Biol. Chem.* 267: 17588-97
 28. Froland WA, Andersson KK, Lee S-K, Liu Y, Lipscomb JD. 1993. The catalytic cycle of methane monooxygenase and the novel roles played by protein component complexes during turnover. See Ref. 46a, pp. 81-92
 29. Froland WA, Dyer D, Radhakrishnan R, Earhart C, Lipscomb JD, Ohlendorf DH. 1994. Preliminary crystallographic analysis of methane monooxygenase hydroxylase from *Methylosinus trichosporium* OB3b. *J. Mol. Biol.* 236: 379-80
 30. Green J, Dalton H. 1989. Substrate specificity of soluble methane monooxygenase: mechanistic implications. *J. Biol. Chem.* 264:17698-17703
 31. Groves JT, McClusky GA, White RE, Coon MJ. 1978. Aliphatic hydroxylation by highly purified liver microsomal cytochrome P-450. Evidence for a carbon radical intermediate. *Biochem. Biophys. Res. Commun.* 81:154-60
 32. Hendrich MP, Fox BG, Andersson KK, Debrunner PG, Lipscomb JD. 1992. Ligation of the diiron site of the hydroxylase component of methane monooxygenase: an ENDOR study. *J. Biol. Chem.* 267:261-69
 33. Hendrich MP, Münck E, Fox BG, Lipscomb JD. 1990. Integer spin EPR studies of the fully reduced methane monooxygenase hydroxylase component. *J. Am. Chem. Soc.* 112:5861-65
 34. Higgins IJ, Best DJ, Hammond RC. 1980. New findings in methane-utilizing bacteria highlight their importance in the biosphere and their commercial potential. *Nature* 286:561-64
 35. Hrycay EG, Gustafsson JÅ, Ingelman-Sundberg M, Ernster L. 1975. Sodium periodate, sodium chlorite, organic hydroperoxides, and H_2O_2 as hydroxylating agents in steroid hydroxylation reactions catalyzed by partially purified cytochrome P-450. *Biochem. Biophys. Res. Commun.* 66:209-16
 36. Jollie DR, Lipscomb JD. 1991. Formate dehydrogenase from *M. trichosporium* OB 3b: purification and spectroscopic characterization of the cofactors. *J. Biol. Chem.* 266:21853-63
 - 36a. Kelly JW, ed. 1991. *Applications of Enzyme Biotechnology*. New York: Plenum
 37. Lee S-K, Fox BG, Froland WA, Lipscomb JD, Münck E. 1993. A transient intermediate of the methane monooxygenase catalytic cycle containing an Fe(IV) \bullet Fe(IV) cluster. *J. Am. Chem. Soc.* 115:6450-51
 38. Lee S-K, Nesheim JC, Lipscomb JD. 1993. Transient intermediates of the methane monooxygenase catalytic cycle. *J. Biol. Chem.* 268:21569-77
 39. Leising RA, Brennen BA, Que L Jr,

- Fox BG, Münck E. 1991. Models for non-heme iron oxygenases: a high-valent iron-oxo intermediate. *J. Am. Chem. Soc.* 113:3988-90
40. Leising RA, Norman RE, Que L Jr. 1990. Alkane functionalization by non-porphyrin iron complexes: mechanistic insights. *Inorg. Chem.* 29:2553-55
41. Liu K, Johnson CC, Newcomb M, Lippard SJ. 1993. Radical clock substrate probes and kinetic isotope studies of the hydroxylation of hydrocarbons by methane monooxygenase. *J. Am. Chem. Soc.* 115:939-47
42. Liu K, Lippard SJ. 1991. Redox properties of the hydroxylase component of methane monooxygenase from *Methylococcus capsulatus* Bath: effects of protein B, reductase, and substrate. *J. Biol. Chem.* 266:12836-39
43. Liu K, Lippard SJ. 1991. Correction to: redox properties of the hydroxylase component of methane monooxygenase from *Methylococcus capsulatus* Bath: effects of protein B, reductase, and substrate. *J. Biol. Chem.* 266:24859
44. McMurry TJ, Groves JT. 1986. Metalloporphyrin models for cytochrome P-450. In *Cytochrome P-450 Structure, Mechanism, and Biochemistry*, ed. PR Ortiz de Montellano, pp. 1-28. New York: Plenum
45. Miller RE, Guengerich FP. 1982. Oxidation of trichloroethylene by liver microsomal cytochrome P-450: evidence for chlorine migration in a transition state not involving trichloroethylene oxide. *Biochemistry* 21:1090-97
46. Münck E. 1978. Mössbauer spectroscopy of proteins: electron carriers. *Methods Enzymol.* 54:346-79
- 46a. Murrell JC, Kelly DP, eds. 1993. *Microbial Growth on C₁ Compounds*. Andover UK: Intercept
47. Nakajima T, Uchiyama H, Yagi O, Nakahara T. 1992. Purification and properties of a soluble methane monooxygenase from *Methylocystis* sp. M. *Biosci. Biotech. Biochem.* 56:736-40
48. Nicolaidis AA, Sargent AW. 1987. Isolation of methane monooxygenase mutants from *Methylosinus trichosporium* OB3b using dichloromethane. *FEMS Microbiol. Lett.* 41:47-52
49. Nordlund P, Dalton H, Eklund H. 1992. The active site structure of methane monooxygenase is closely related to the binuclear iron center of ribonucleotide reductase. *FEBS Lett.* 307:257-62
50. Nordlund P, Sjöberg B-M, Eklund H. 1990. Three-dimensional structure of the free radical protein of ribonucleotide reductase. *Nature* 345:593-98
51. Nunn DN, Day D, Anthony CC. 1989. The second subunit of methanol dehydrogenase of *Methylobacterium extorquens* AM1. *Biochem. J.* 260:857-62
52. Patel RN, Savas JC. 1987. Purification and properties of the hydroxylase component of methane monooxygenase. *J. Bacteriol.* 169:2313-17
53. Paulsen KE, Liu Y, Fox BG, Lipscomb JD, Münck E, Stankovich MT. 1994. EPR-spectroelectrochemical studies of the methane monooxygenase hydroxylase component from *Methylosinus trichosporium* OB3b: redox potential determinations of the hydroxylase component alone and complexed to component B. *Biochemistry.* 33:713-22
54. Petersson L, Gräslund A, Ehrenberg A, Sjöberg B-M, Reichard P. 1980. The iron center in ribonucleotide reductase from *Escherichia coli*. *J. Biol. Chem.* 255:6706-12
55. Pilkington SJ, Dalton H. 1990. Soluble methane monooxygenase from *Methylococcus capsulatus* Bath. *Methods Enzymol.* 188:181-90
56. Priestley ND, Floss HG, Froland WA, Lipscomb JD, Williams PG, Morimoto H. 1992. Cryptic stereospecificity of methane monooxygenase. *J. Am. Chem. Soc.* 114:7561-62
57. Pulver S, Froland WA, Fox BG, Lipscomb JD, Solomon EI. 1993. Spectroscopic studies of the coupled binuclear non-heme iron active site in the fully reduced hydroxylase component of methane monooxygenase: comparison to deoxy and deoxy-azide hemerythrin. *J. Am. Chem. Soc.* 115:12409-22
58. Rataj MJ, Kauth JE, Donnelly MI. 1991. Oxidation of deuterated compounds by high specific activity methane monooxygenase from *Methylosinus trichosporium*: mechanistic implications. *J. Biol. Chem.* 266:18684-90
- 58a. Rosenzweig AC, Frederick CA, Lippard SJ, Nordlund P. 1993. Crystal structure of a bacterial non-haem iron hydroxylase that catalyzes the biological oxidation of methane. *Nature* 336:537-43
59. Rusicka F, Huang D-S, Donnelly MI, Frey PA. 1990. Methane monooxygenase catalyzed oxygenation of 1,1-dimethylcyclopropane. Evidence for radical and carbocationic intermediates. *Biochemistry* 29:1696-1700
60. Solomon EI, Zang Y. 1992. The electronic structures of active sites in non-heme iron enzymes. *Acc. Chem. Res.* 25:343-52
61. Stanley SH, Prior SD, Leak DJ, Dalton H. 1983. Copper stress underlies the fundamental change in intracellular lo-

- cation of methane monooxygenase in methane-oxidizing organisms: studies in batch and continuous cultures. *Biotech. Lett.* 5:487-92
62. Stenkamp RE, Sieker LC, Jensen LH, McCallum JD, Sanders-Loehr J. 1985. Active site structures of deoxyhemerythrin and oxyhemerythrin. *Proc. Natl. Acad. Sci. USA* 82:713-67
63. Thomann H, Bernardo M, McCormick JM, Pulver S, Andersson KK, et al. 1993. Pulsed EPR studies of mixed valent [Fe(II)Fe(III)] forms of hemerythrin and methane monooxygenase: evidence for a hydroxide bridge. *J. Am. Chem. Soc.* 115:8881-82
64. Tsien HC, Brusseau GA, Hanson RS, Wackett LP. 1989. Biodegradation of trichloroethylene by *Methylosinus trichosporium* OB3b. *Appl. Environ. Microbiol.* 55:3155-61
65. Vincent JB, Olivier-Lilley GL, Averill BA. 1990. Proteins containing oxo-bridged dinuclear iron centers: a bioinorganic perspective. *Chem. Rev.* 90:1447-67
66. Whittenbury R, Phillips KC, Wilkinson JF. 1970. Enrichment, isolation and some properties of methane-utilizing bacteria. *J. Gen. Microbiol.* 61:205-18
67. Woodland MP, Dalton H. 1984. Purification and characterization of component A of the methane monooxygenase from *Methylococcus capsulatus* Bath. *J. Biol. Chem.* 259:53-59
68. Woodland MP, Patil DS, Cammack R, Dalton H. 1986. ESR studies of protein A of the soluble methane monooxygenase from *Methylococcus capsulatus* Bath. *Biochim. Biophys. Acta* 873:237-42
69. Xia Z-X, Dai W-W, Xiong J-P, Hao Z-P, Davidson VL, et al. 1992. The three dimensional structures of methanol dehydrogenase from two methylophilic bacteria at 2.6 Å resolution. *J. Biol. Chem.* 267:22289-97